Larhyss Journal, ISSN 1112-3680, n°52, Dec 2022, pp. 76-92

ANALYTICAL APPROACH OF TWO GENERAL NONLINEAR SHIP MOTIONS IN TIME DOMAIN

REKHA S.[1], GOWTHAMAN D.[2], BALAGANESAN P.[3*], ACHOUR B.[4]

[1,2] Research Scholar, Department of Mathematics, AMET Deemed to be University, Chennai, Tamil Nadu, India
[3] Associate Professor, Department of Mathematics, AMET Deemed to be University, Chennai, Tamil Nadu, India
[4] Professor, Research Laboratory in Subterranean and Surface Hydraulics (LARHYSS) University of Biskra, Algeria

(*) balaganesan.p@ametuniv.ac.in

Research Article – Available at http://larhyss.net/ojs/index.php/larhyss/index
Received August 5, 2022, Received in revised form December 2, 2022, Accepted December 4, 2022

ABSTRACT

Two nonlinear models of the roll motion of ships are discussed and analytically solved. Both models are second-order differential equations with nonlinear restoring and damping moments. A new approach to the homotopy perturbation method is applied to derive analytical expressions for the roll angle, velocity, acceleration and restoring and damping moments. The analytical results are validated by direct comparison with the fourth-order Runge–Kutta method. The analytical approach of this paper can be efficiently extended to various vibrating dynamical models arising in mechanical systems.

Keywords: Mathematical modeling, ship dynamics, capsizing, restoring and damping moments, analytical solution.

INTRODUCTION

Generally, ships are subjected to three types of displacement motions (heave, sway and surge) in addition to three angular motions (yaw, pitch, and roll), as depicted in Figure 1. Equations of motion are based on either Lagrange’s equation or Newton’s second law (Ibrahim et al., 2010).

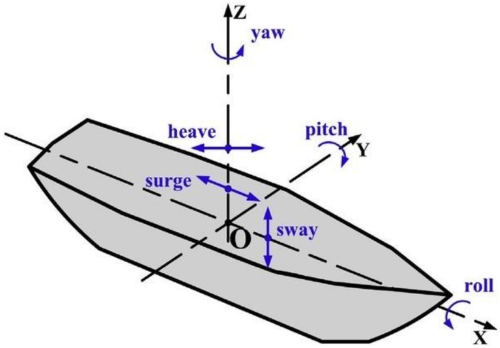

Figure 1: Schematic diagram of a ship showing the six degrees of freedom

An accurate prediction of a ship's roll motion is essential for the design of dynamic stability, which relies on the precision of calculating nonlinear roll damping properties (Jang et al., 2010). To that end, the literature has been intensively enriched with investigations of the roll motion of ships over the past few decades. Wilson et al. (2006) developed an unsteady RANS method for the viscous phenomenon of roll decay motion for a surface combatant (Wilson et al., 2006, Falzarano et al., 1992) and used global analysis techniques to study the transient rolling motions of a small ship that is subjected to periodic wave excitation.

Numerical and analytical studies that aim at predicting a ship roll motion are important and complement each other even though there is a dispute about which of the two serves as a preliminary to the other. Many numerical approaches usually start by "guessing" an initial solution and then iteratively refine the solution until a previously defined error metric is minimized. The heavy computational effort for this task may be dramatically reduced by choosing better "initial guesses". With a reliable analytical solution, this could be easily achieved. In the field of computer science (neuronal networks), the clever choice of initial start parameters has shown large performance improvements. With the analytical solution, however, similar improvements could also be expected for the simulation roll motion. However, although numerical solutions are efficiently obtained, there are some pitfalls that make many engineers and applied scientists prefer analytical solutions if they can be obtained. The most serious pitfalls that come with numerical solutions are numerical stabilities, and adjusting parameters to match the numerical data may be extremely difficult to achieve (Devi et al., 2020).

Both analytical and numerical studies of roll motion are essential for the investigation of parametric rolling of ships, which can build up to high roll angles and possibly lead to capsizing. For example, Hamamoto et al. (1996) performed an analytical study to identify the occurrence of a critical condition leading to the capsize phenomenon for a container ship due to parametric rolling. However, (Munif et al., 2000) performed several numerical simulations to validate a six-degree-of-freedom nonlinear model to study the parametric roll and capsizing limits for a ship in the Arctic Sea. Ghamari et al. (2020) performed both numerical and experimental investigations to study the parametric resonance in roll motion for a fishing vessel in regular waves.

Mathematical modeling of marine vessels is under continuous development to keep up with new requirements of marine ship design, maneuvering, operation and safety. While the models become more complicated in terms of stronger nonlinearity damping terms, the development of new efficient numerical and analytical schemes makes it possible to simulate the ship response traveling with a complicated environmental disturbance (Xu et al., 2019). Hou et al. (2018) identified a roll motion equation for floating structures in irregular waves using a combination of the random decrement technique and support vector regression. Kawahara et al. (2011) used Ikeda's method to calculate the roll damping of various ship hulls with various bilge keels. (Xu et al., 2019) used the least squares method followed by singular value decomposition to estimate the uncertainty of the hydrodynamic coefficients of a nonlinear maneuvering model based on planar motion mechanism tests. For more recently published relevant work, see (Mitra et al., 2018; Dashtimanesh et al., 2019; Sun et al., 2019).

In this paper, two general nonlinear dynamic models of ship motion are analytically discussed. One is a nonlinear dynamical system with a single degree of freedom of a ship of free decay, and the other is quadratic roll damping with a nonlinear restoring function. A new version of the homotopy perturbation method is employed to derive analytical expressions for the roll angle, velocity and restoring and damping moments for each model.

MATHEMATICAL FORMULATION OF THE PROBLEM

A typical equation representing a nonlinear ship rolling motion of a free decay is given by

$$(\mathrm{I} + \mathrm{A})\ddot{\mathrm{x}} + \varepsilon\,\mathrm{F}(\mathrm{x}, \dot{\mathrm{x}}) + \mathrm{G}(\mathrm{x}) = 0 \tag{1}$$

where x is the roll angle, I is the roll inertia moment, A is the added inertia moment, $\epsilon\,\mathrm{F}(\mathrm{x}, \dot{\mathrm{x}})$ is a nonlinear damping moment in which ε is a perturbation expansion parameter and $\mathrm{G}(\mathrm{x})$ is a nonlinear restoring moment. The first term represents the force of inertia, and the second and third terms describe the moments of damping and regeneration. Dividing by $(I + A)$, we obtain the normalized form (Sun et al., 2019).

$$\ddot{x} + g(x) = \varepsilon f(x, \dot{x}) \tag{2}$$

where the nonlinear functions $\mathrm{g(x)}$ and $\varepsilon \mathrm{f}(\mathrm{x}, \dot{\mathrm{x}})$ are the new restoring and damping moments, respectively.

ANALYTICAL EXPRESSION OF ROLL ANGLE AND VELOCITY

As an exact solution of the nonlinear governing equation of the roll motion is almost impossible to find, the search for approximate numerical or experimental solutions is a necessity. There are many numerical and analytical methods that are prone to producing reliable approximate solutions and have been employed by many researchers in various fields of engineering and sciences. Of the numerical methods, the finite difference method (Tirmizi et al., 2002) includes weighted residual numerical methods such as spectral methods (Bhrawy et al., 2013), wavelet-based methods (Abualrub et al., 2015), and spline-based methods (Abukhaled et al., 2011). Among the analytical methods that have proven to be very effective in solving nonlinear initial-boundary value problems, we mention the variational iteration method (He, 2007; Wazwaz, 2013; Abukhaled 2013), Adomian decomposition method (Duan et al., 2015), homotopy analysis method (Liao et al., 2012), Green's function-based method (Abukhaled et al., 2020), and differential transformation method (Hassan et al., 2008).

One of the most effective analytical methods and most used in the last two decades is the homotopy perturbation method (HPM). First introduced by He (1999), HPM has encountered many modifications to encompass a wide range of nonlinear models that have arisen in physical, chemical and engineering sciences (He, 2000, Biazar 2008, Swaminathan 2020, Saravanakumar 2020 and Wassermann 2016. In the next two subsections, we employ a new form of the HPM to derive approximate analytical solutions of the dynamics of roll motions.

A nonlinear system with a single degree of freedom

The second-order nonlinear dynamic system with a single degree of freedom for roll motion is governed by (Hariharan et al., 2016).

$$\frac{d^2x}{dt^2} + \left(2\alpha_1 + \alpha_2 \left|\frac{dx}{dt}\right|\right) \left|\frac{dx}{dt}\right| + \beta_1 x + \beta_3 x^3 + \beta_5 x^5 = 0 \tag{3}$$

With initial conditions,

$$x(0) = 1,\ x'(0) = 0 \tag{4}$$

We construct the homotopy for Eq. (3) as follows:

$$(1-p)\left(\frac{d^2x(t)}{dt^2}\right) + 2\alpha_1 \frac{dx(t)}{dt} + \beta_1 x(t) \tag{5}$$

where $\boldsymbol{P} \in [\mathbf{0}, \mathbf{1}]$ is an embedding parameter. The approximate homotopy solution is expressed in series form

$$x(t) = x_0(t) + p x_1(t) + p^2 x_2(t) + \cdots \tag{6}$$

Substituting Eq. (6) into Eq. (5) and equating like powers of $\boldsymbol{p}$ leads to the linear system

$$p^0: \frac{d^2x_0(t)}{dt^2} + 2\alpha_1 \frac{dx_0(t)}{dt} + \beta_1 x_0(t) = 0 \quad (7)$$

$$p^1: \frac{d^2x_1(t)}{dt^2} + 2\alpha_1 \frac{dx_1(t)}{dt} + \beta_1 x_1(t) + 2\alpha_2 \left(\frac{dx_0(t)}{dt}\right)^2 + \beta_3\big(x_0(t)\big)^3 + \beta_5\big(x_0(t)\big)^5 = 0 \quad (8)$$

Subject to initial conditions

$$x_0(0) = 1,\ x_0{}'(0) = 0 \quad (9)$$

$$x_1(0) = 0,\ x_1{}'(0) = 0 \quad (10)$$

Solving systems (7) to (10) gives a two-term HPM analytical expression for the roll angle $x(t)$ from which the analytical expressions of the velocity, acceleration, and restoring and damping moments are, respectively, given by the following:

$$\text{Velocity} = \frac{dx(t)}{dt} \quad (11)$$

$$\text{Accelearation} = \frac{dx^2(t)}{dt^2} \quad (12)$$

$$\text{Restoring momrnt } r\big(x(t)\big) = \beta_1\big(x(t)\big) + \beta_3\big(x(t)\big)^3 + \beta_5\big(x(t)\big)^5 \quad (13)$$

$$\text{Damping moment} = \alpha_1 \frac{dx(t)}{dt} + \alpha_1 \left(\frac{dx(t)}{dt}\right)^2 \quad (14)$$

Quadratic roll damping with nonlinear restoring function

The quadratic roll damping with the nonlinear restoring function was given by the following (Bass et al., 1988)

$$\frac{d^2x}{dt^2} + 2\omega\varsigma \left(\frac{dx}{dt} + \varepsilon \left|\frac{dx}{dt}\right| \frac{dx}{dt}\right) + \omega^2(x + \mu x^3) = 0 \quad (15)$$

Subject to initial conditions:

$$x(0) = 1,\ x'(0) = 0 \quad (16)$$

To analytically solve Eqs. (15) using (16), we begin by constructing the homotopy as follows:

$$1 - p\left(\frac{d^2x(t)}{dt^2} + 2\omega\varsigma\frac{dx}{dt} + \omega^2 x(t)\right) + p\left(\frac{d^2x(t)}{dt^2}\right) + 2\omega\varsigma\frac{dx}{dt} + 2\omega\varepsilon\varsigma\left(\frac{dx}{dt}\right)^2 + \omega^2 x(t) + \omega^2\mu\big(x(t)\big)^3 = 0 \quad (17)$$

where $P \in [0,1]$ is an embedding parameter. Substituting the series solution given by (6) into Eq. (17) and equating like powers of p leads to the linear system

$$p^0: \left(\frac{d^2x_0(t)}{dt^2} + 2\omega\varsigma\frac{dx_0(t)}{dt} + \omega^2\big(x_0(t)\big)\right) = 0 \quad (18)$$

$$p^1: \left(\frac{d^2x_1(t)}{dt^2} + 2\omega\varsigma\frac{d1(t)}{dt} + \omega^2\big(x_1(t)\big) + 2\omega\varepsilon\varsigma\left(\frac{dx_0(t)}{dt}\right) + \omega^2\mu(x_0(t))^3\right) = 0 \qquad (19)$$

Solving systems (18) and (19) subject to initial conditions (9) and (10) and substituting the results into Eq. (6) and then taking the limit as $p \rightarrow 1$ gives a two-term HPM solution. The velocity, acceleration and damping and restoring moments are obtained as in (11) - (14).

NUMERICAL EXAMPLES AND DISCUSSION

Example 1

Consider systems (3) - (4) with the following experimental values:

$$\alpha_1 = 0.02,\ \alpha_2 = 0.002,\ \beta_1 = 0.3948,\ \beta_3 = 0.3948 \times 10^{-4},\ \beta_5 = 0.3948 \times 10^{-4},\ l = 1 \qquad (20)$$

$$x(t) = 0.00025\, cos(0.62802x - 1.6662)e^{-0.1x} + \big(0.000315\cos(1.8841x - 0.14326) + 0.059\, cos(0.62802x - 1.6345)\big)\, e^{-0.06x} + \big(-0.002 + 0.00067\, cos(1.256x + 3.0991)\big)e^{-0.01x} + 1.0065\, e^{-0.02x}\, cos(0.62802x + 0.02749) \qquad (21)$$

To test the accuracy of solution (20), it will be compared to the solution obtained by the Chebyshev wavelet method (CWM) (G. Hariharan 2016) and a fourth-order Runge–Kutta numerical solution (RK4). Table I shows that the proposed analytical expression for the roll angle (G. Hariharan 2016) is in much stronger agreement with the RK4 solution than the CWM.

Table 1: Comparison between the proposed method, CWM, and RK4 for the roll angle Eq. (20)

Time (s)	Roll angle $x(t)$			Absolute Error	
	Proposed (HPM)	CWM [32]	Numerical	Proposed (HPM)	CWM [32]
0.0	0.99996	1.00000	1.000000000	0.000040000	0.000000000
0.1	0.99799	0.99813	0.998009389	0.000019389	0.000120610
0.2	0.99204	0.99254	0.992056171	0.000016171	0.000483830
0.3	0.98216	0.98321	0.982180128	0.000020128	0.001029900
0.4	0.96842	0.97014	0.968436675	0.000016675	0.001703300
0.5	0.95087	0.95335	0.950896513	0.000026513	0.002453500
0.6	0.92962	0.93282	0.929645322	0.000025322	0.003174700
0.7	0.90477	0.90857	0.904783218	0.000013218	0.003786800
0.8	0.87641	0.88058	0.876424358	0.000014358	0.004155600
0.9	084468	0.84885	0.844696325	0.000016325	0.004153700
1.0	0.80972	0.81340	0.809739454	0.000019545	0.003660500

Moreover, the proposed analytical solution maintains a strong convergence rate and stability over a very large time domain, while the Chebyshev wavelet method starts to diverge as soon as t increases beyond 1, as shown in Fig. 2 and Fig. 3.

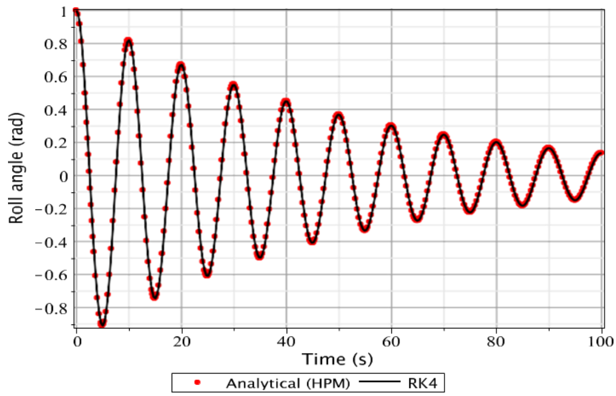

Figure 2: Comparison between the analytical and numerical roll angle curves of Eq. (20).

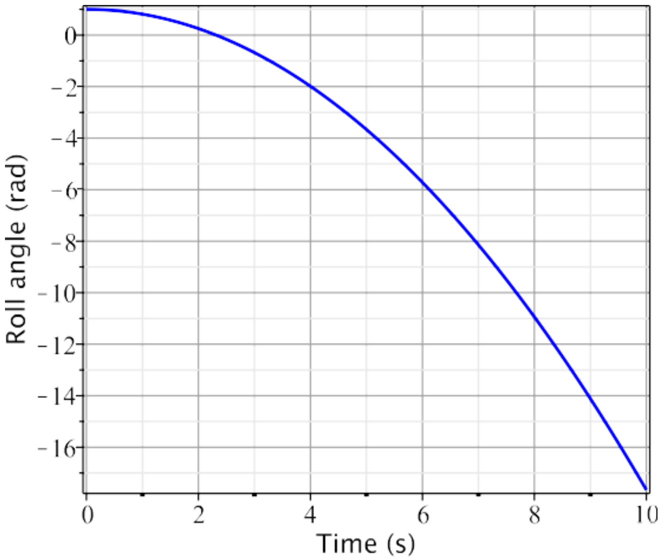

Figure 3: Chebyshev roll angle curve of Eq. (20) showing divergence for *t* larger than 1.

Fig. 4 shows that the velocity obtained analytically using the proposed HPM is in strong agreement with RK4 and remains stable over a large time interval.

Figs. 5 and 6 depict the restoring and damping moment curves, respectively, with comparisons to the numerical RK4 curves.

Figs. 5 and 6 depict the restoring and damping moment curves, respectively, with comparisons to the numerical RK4 curves.

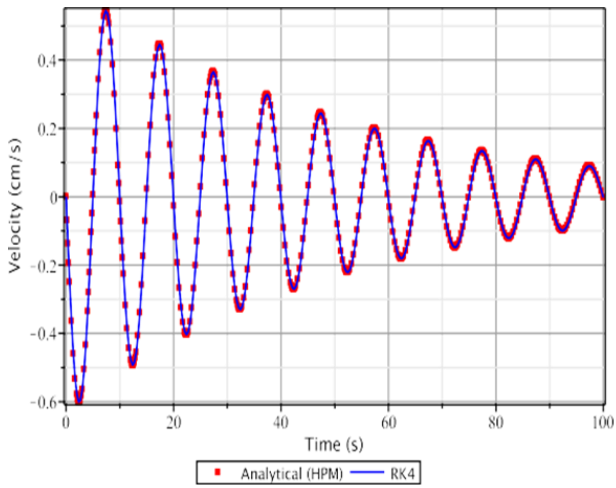

Figure 4: Comparison between the analytical and numerical velocity curves for Example 1.

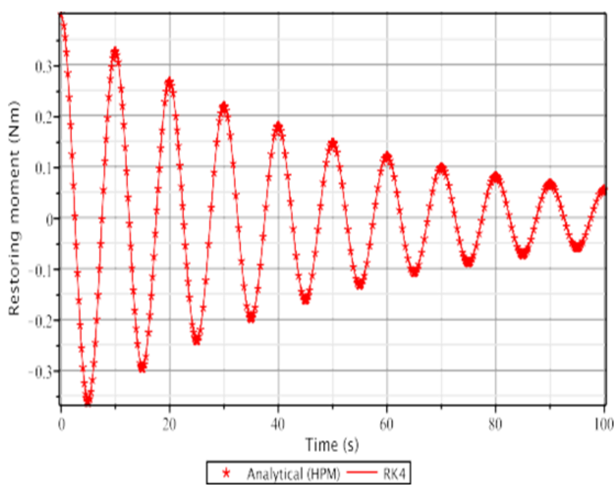

Figure 5: Analytical and numerical restoring moment curves for Example 1

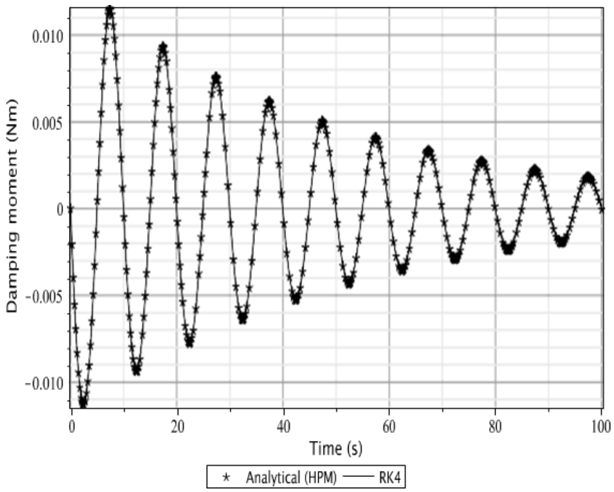

Figure 6: Analytical and numerical damping moment curves for Example 1

Example 2

Consider systems (15)-(16) with the following experimental values (He, 2007):

$$\omega = 5,\ \varsigma = 0.02,\ \varepsilon = 1,\ \mu = 0.5,\ l = 0.25 \quad (22)$$

The two-term homotopy solution from Eq. (18) - (19), which represents the roll angle, is given by

$$x(t) = \big(0.3475\, cos(4.999x - 1.6108) + 0.00116\, cos(14.997x - 0.09001)\big)e^{-0.3x} + \big(-0.01765 + 0.00588\, cos(9.998x + 3.11492)\big)e^{-0.2x} + 0.5689\, e^{-0.1x}\, cos(4.999x + 0.64011) \quad (23)$$

Table 2 shows that the proposed analytical solution of the roll angle is in strong agreement with the numerical RK4 solution. Figures 7 and 8 show that the roll angle and velocity curves maintain a high rate of accuracy and stability over a large interval domain.

Tables 1 and 2 show that the analytical and numerical solutions for the roll angle and the velocity are instrong agreement when t is sufficiently close to the initial value. Figs. 6 and 7 show the analytical and numerical roll angle and velocity curves versus time. It is clear that as time moves far away from the initial point 0, the analytical curves deviate from the numerical curves, as expected, but this deviation isstill small, and most importantly, the analytical curves maintain stability.

Table 2: Comparison between the proposed method and RK4 for the roll angle Eq. (22)

Time (s)	Proposed (HPM)	Numerical	Absolute error
0.00	0.250000000	0.250000000	0.000000000
0.10	0.218642955	0.218640722	0.000002233
0.20	0.132910553	0.132873544	0.000037008
0.30	0.014275399	0.014090036	0.000185363
0.40	-0.108215489	-0.108722581	0.000507092
0.50	-0.204127183	-0.204974034	0.000846851
0.60	-0.248869957	-0.279683043	0.000813086
0.70	-0.231125751	-0.231375118	0.000249366
0.80	-0.156876496	-0.156454489	0.000422007
0.90	-0.047043835	-0.046355431	0.000688405
1.00	0.069748126	0.070245472	0.000497345

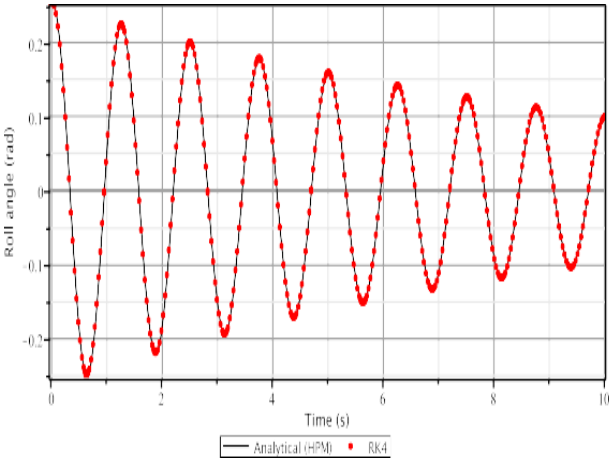

Figure 7: Comparison between the analytical and numerical roll angle curves of Eq. (22).

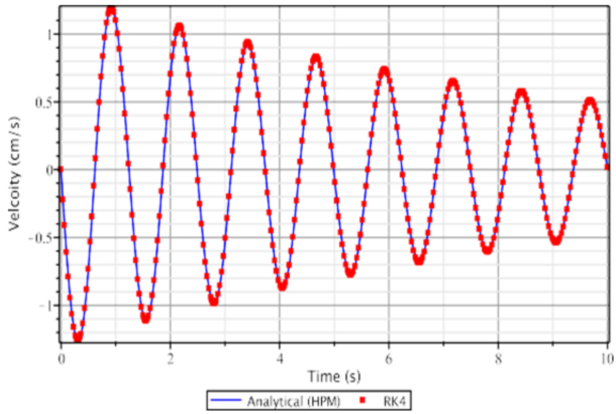

Figure 8: Comparison between the analytical and numerical velocity curves for Example 2

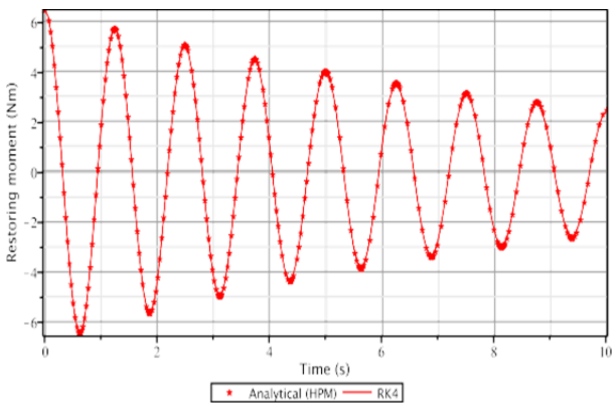

Figure 9: Analytical and numerical restoring moment curves for Example 2

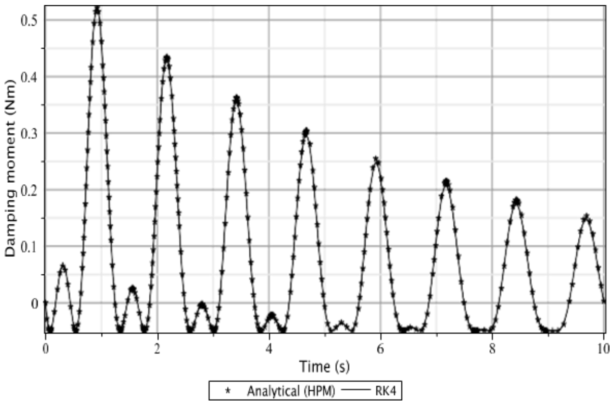

Figure 10: Analytical and numerical damping moment curves for Example 2

Figures 9 and 10 depict the analytical and numerical curves of the restoring and damping moments, respectively.

From the rolling curves (Figs. 2 and 7) and their corresponding velocity curves (Figs. 4 and 8), it is inferred that the roll angle always decreases rapidly with time. This rapid decline is due to the initial roll angle and then stable roll response patterns at the wave periods. The roll damping coefficients are determined using the logarithmic decrement method using the first two peaks of the roll decay curve. The damping ratio and natural frequency are obtained using the following equations from the logarithmic decrement process (Wazwaz et al., 2013).

$$\delta = I_n\left(\frac{\phi_1}{\phi_2}\right),\ \xi = \sqrt{1+\left(\frac{2\pi}{d}\right)^2},\ T_n = dT\sqrt{1-\xi^2} \tag{24}$$

where δ is the logarithmic decrement, $\varphi 1$ and $\varphi 2$ are the two successive roll amplitudes, ξ is the roll damping ratio, T_n is the roll natural period and dT is the time difference between two successive roll amplitudes.

The maximum amplitude of the roll motion of these two models depends upon the initial conditions. In Fig. 11, the black line represents the envelope (line joining the peaks of amplitudes) of the roll decay curves. The equation of the envelopes can be computed from the following equation:

$$envelope = \pm x\ (t=0)e^{-\frac{d}{2}t} \tag{25}$$

where d is the coefficient of dx. For the considered examples 1 and 2, the envelope functions are given by $x(t) = e^{-0.02t}$and$(t) = 0.25\ e^{-0.1t}$, respectively. Note that from these equations, the time for the roll angle to reach a steady state can be computed.

Figs. 11 and 12 show the curves of the roll angle given in examples 1 and 2 along with the envelope curves.

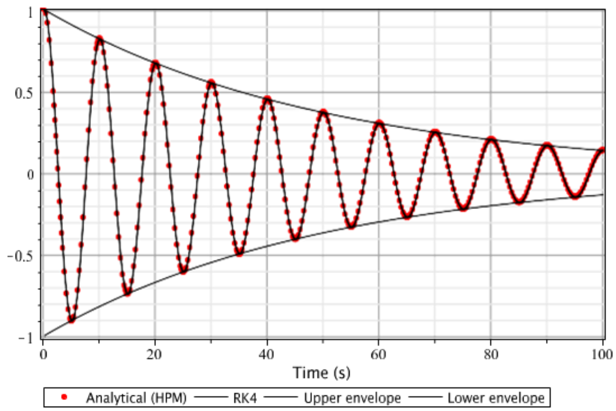

Figure 11: Analytical and numerical roll angle and envelope curves for Example 1

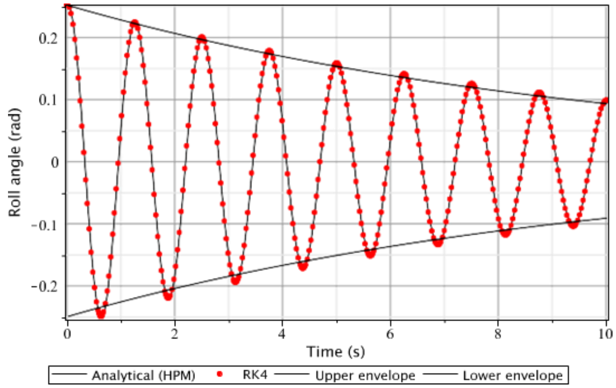

Figure 12: Analytical and numerical roll angle and envelope curves for Example 2

The velocity curves depicted in Figures 4 and 8 show that the peak amplitudes, which are the well-known significant factors of capsizing ships, depend on the initial condition. These amplitudes gradually decrease with time. Figs. 5, 6, 9 and 10 also show that the moments of regeneration and damping also decrease as time increases. These figures also show a nonlinear effect on the roll moment and stress around the hull by the width of the bilge keel. Bilge keels affect roll damping mainly through the quadratic component of roll damping.

CONCLUSIONS

Two nonlinear second-order equations used as models for ship motions are analytically solved to predict roll damping. The analytical decay curves are obtained using a simple approach of the homotopy perturbation method. The obtained approximate analytical results are shown to be in strong agreement with the numerical RK4 results. The simple closed-form analytical results can be used for data processing, identification of parameters and roll damping coefficients. The extension of the proposed approach is possible in three or several degrees of freedom for nonlinear ship motion of heave and pitch.

REFERENCES

ABUALRUB T., ABUKHALED M. (2015). Wavelets approach for optimal boundary control of cellular uptake in tissue engineering, International Journal of Computer Mathematics, Vol. 92, Issue 7, pp. 1402-1412.

ABUKHALED M., KHURI S., SAYFY A. (2011). A numerical approach for solving a class of singular boundary value problems arising in physiology, International Journal of Numerical Analysis and Modeling, Vol. 8, Issue 2, pp. 353-363.

ABUKHALED M., KHURI S. (2020). Efficient numerical treatment of a conductive-radiative fin with temperature dependent thermal conductivity and surface emissivity, International Journal for Computational Methods in Engineering Science and Mechanics, Vol. 21, Issue 4, pp. 159-168.

ABUKHALED M. (2013). Variational iteration method for nonlinear singular two-point boundary value problems arising in human physiology, Journal of Mathematics, Article 720134.

BASS DW., HADDARA MR. (1988). Nonlinear models of ship roll damping. International Shipbuilding Progress, Vol. 35, Issue 401, pp. 5-24.

BHRAWY A. (2013). A Jacobi-Gauss-Lobatto collocation method for solving generalized Fitzhugh-Nagumo equation with time-dependent coefficients, Applied Mathematics and Computation, Vol. 222, Issue 1, pp. 255-264.

BIAZAR J., GHAZVINI H. (2008). Homotopy perturbation method for solving hyperbolic partial differential equations, Computers and Mathematics Applications Vol. 56, Issue 2, pp. 453-458.

DASHTIMANESH A., ENSHAEI H., TAVAKOLI S. (2019). Oblique-asymmetric 2D1T model to compute hydrodynamic forces and moments in coupled sway, roll, and yaw motions of planning hulls, Journal of Ship Research, Vol. 63, Issue 1, pp. 1-15.

DUAN J-S., RACH R., WAZWAZ A.M. (2015). A reliable algorithm for positive solutions of nonlinear boundary value problems by the multistage Adomian decomposition method, Open Engineering, Vol. 5, Issue 1, pp. 59-74.

FALZARANO J., SHAW S., TROESCH A. (1992). Application of global methods for analyzing dynamical systems to ship rolling motion and capsizing. International Journal of Bifurcation and Chaos, Vol. 2, Issue 1, pp. 101-115.

GHAMARI I., GRECO M., FALTINSEN O., LUGNI C. (2020). Numerical and experimental study on the parametric roll resonance for a fishing vessel with and without forward speed, Applied Ocean Research, Vol. 101, Article 102272.

HAMAMOTO M., PANJAITAN J. (1996). A critical situation leading to capsize of ships in astern seas, Journal of the Society of Naval Architects of Japan, Vol. 1996, Issue 180, pp. 215-221.

HARIHARAN G., RAJARAMAN R., SATHIYASEELAN D. (2016). Wavelet based spectral algorithm for nonlinear dynamical systems arising in ship dynamics, Ocean Engineering**,** Vol. 126, pp. 321-328.

HASSAN I. (2008). Application to differential transformation method for solving systems of differential equations, Applied Mathematical Modelling, Vol. 32, Issue 12, pp. 2552-2559.

HE J.H. (1999). Homotopy perturbation technique, Computer Methods in Applied Mechanics and Engineering, Vol. 178, Issue 3-4, pp. 257-262.

HE J.H. (2007). Variational iteration method-some recent results and new interpretations, Journal of Computational and Applied Mathematics, Vol. 207, Issue 1, pp. 3-17.

IBRAHIM R.A., GRACE I.M. (2010). Modeling of ship roll dynamics and its coupling with heave and pitch, Mathematical Problems in Engineering, Vol. 2010, Article ID 934714, pp. 1-31.

JANG T.S., KWON S.H., LEE. J.H. (2010). Recovering the functional form of the nonlinear roll damping of ships from a free-roll decay experiment: An inverse formulism, Ocean Engineering, Vol. 37, Issue 13-14, pp. 1337-1344.

KAWAHARA Y., MAEKAWA K., IKEDA Y. (2011). A simple prediction formula of roll damping of conventional Cargo ships on the basis of Ikeda's method and its limitation, Fluid Mechanics and Its Applications, Vol. 97, pp. 465–486.

LIAO S.J. (2012). Homotopy analysis method in nonlinear differential equations, Springer and Higher Education Press, Heidelberg, Shanghai, China.

MITRA R.K., BANIK A.K., DATTA T.K., CHATTERJEE S. (2018). Nonlinear roll oscillation of semisubmersible system and its control, International Journal of Non-Linear Mechanics, Vol. 107, pp. 42-55.

MUNIF A., UMEDA N. (2000). Modeling extreme roll motions and capsizing of a moderate-speed ship in astern waves, Journal of the Society of Naval Architects of Japan, Vol. 187, 2000, pp. 51-58.

SUN S., SHAO M. (2019). Estimation of nonlinear roll damping by analytical approximation of experimental free-decay amplitudes, Journal of Ocean University of China, Vol. 18, pp. 812-822.

TIRMIZI I., TWIZELL E. (2002). Higher-order finite-difference methods for nonlinear second-order two-point boundary-value problems, Applied Mathematics Letters, Vol. 15, Issue 7, pp. 897-902.

WASSERMANN S., FEDER D.F., ABDEL-MAKSOUD M. (2016). Estimation of ship roll damping-A comparison of the decay and the harmonic excited roll motion technique for a post panamax container ship, Ocean Engineering, Vol. 120, pp. 371-382.

WAZWAZ A.M. (2013). A reliable iterative method for solving the time-dependent singular Emden-Fowler equations, Central European Journal of Engineering, Vol. 3, Issue 1, pp. 99-105.

WILSON P., CARRICA P., STERN F. (2006). Unsteady RANS method for ship motions with application to roll for a surface combatant, Computers and Fluids, Vol. 35, Issue 5, pp. 501-524.

XU H., HASSANI V., GUEDES SOARES C. (2019). Uncertainty analysis of the hydrodynamic coefficient’s estimation of a nonlinear maneuvering model based on planar motion mechanism tests, Ocean Engineering, Vol. 173, Issue 3, pp. 450-459.